EFFECT OF GEOMETRY AND IMPEDANCE VARIATION ON THE ACOUSTIC PERFORMANCE OF A POROUS MATERIAL LINED DUCT

Abdelmonem Masmoudi, Amine Makni, Mohamed Taktak, Mohamed Haddar

Mechanics, Modelling and Production Laboratory (LA2MP), Mechanical Department, National School of Engineers of Sfax,
University of Sfax, Sfax, Tunisia; e-mail: mohamed.taktak@fss.rnu.tn

In this paper, the effect of geometry and impedance on the acoustic behavior of wall and lined cylindrical ducts is investigated using a numerical model which enables one to compute the reflection and the transmission coefficients of such ducts using the multimodal scattering matrix. From this matrix, the acoustic power attenuation is deduced. By using these tools, the effect of duct diameter increase and duct diameter decrease of the wall or lined duct section is studied. The numerical results are obtained for two configurations of wall and lined ducts. Numerical coefficients of transmission and reflection as well as the acoustic power attenuation show the relative influence of each type of variation.

Keywords: cylindrical duct, discontinuity effect, transmission, reflection, acoustic attenuation

1. Introduction

The acoustic performance of duct systems is evaluated with different matrices such as the transfer matrix, the mobility matrix and the scattering matrix. This later showed its efficiency not only because it describes the reflection and the transmission phenomena of the studied duct as presented in Abom (1991), Leroux *et al.* (2003), Bi *et al.* (2006), Sitel *et al.* (2006) and Taktak *et al.* (2010), but also because it describes the energetic state of the duct element as presented in Sitel *et al.* (2006), Taktak *et al.* (2010), Aurégan and Starobinski (1998).

In a previous work, Taktak *et al.* (2010) developed a numerical method based on the finite element method to compute the multimodal scattering matrix of a lined axisymetric duct element to investigate the effect of a locally reacting liner. Then, that numerical method was developed to incorporate the flow effect in Taktak *et al.* (2012, 2013). Finally, Ben Jdidia *et al.* (2014) used the multimodal scattering matrix to evaluate the effect of temperature on acoustic behavior of the duct element lined with porous materials.

In this work, the effect of discontinuities in duct systems is investigated based on the use of the multimodal scattering matrix. This objective is achieved by studying two types of cylindrical ducts having sudden changes of the section. In the present work, it is supposed that these section changes are lined. Then, the effect of geometrical dimensions and the liner on the acoustic performances of the studied ducts is investigated by computing the reflection, transmission coefficients and the acoustic power attenuation of these ducts.

The outline of the paper is as follows. The studied problem and numerical computation of the multimodal scattering matrix are presented in Section 2. Then, the used acoustic impedance to model the liner is presented in Section 3. Section 4 presents the computation of acoustic power attenuation from the multimodal scattering matrix. Finally, numerical results are presented and discussed in Section 5 to evaluate the influence of duct diameter increase or duct diameter decrease effects on the reflection and transmission coefficients and the acoustic power attenuation of the studied ducts.

2. Numerical computation of the multimodal scattering matrix

In this study, a 1 m length cylindrical duct element is studied. Two cases of this duct are investigated:

- The first case, as presented in Fig. 1, is a cylindrical duct with radius R located between the two axial coordinates z_L and z_R and presenting an abrupt stricture of the section between z_1 and z_2 with radius ρ. The length of the duct is divided into three parts: two identical parts with length b and radius R and the third part in the middle with length c and radius ρ.
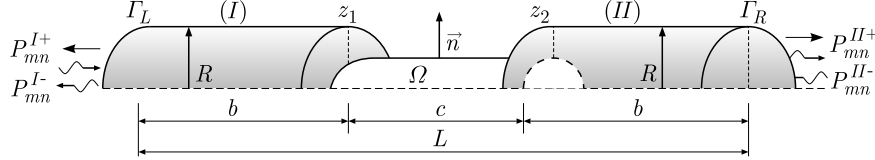

Fig. 1. Section having a duct diameter decrease and then a sudden duct diameter increase section

- The second case, as presented in Fig. 2, is a cylindrical duct with radius ρ located between the two axial coordinates z_L and z_R and presenting an abrupt expansion of the section between z_1 and z_2 with radius R. The length of the duct is divided into three parts: two identical parts with length b and radius ρ and the third part in the middle with length c and radius R.
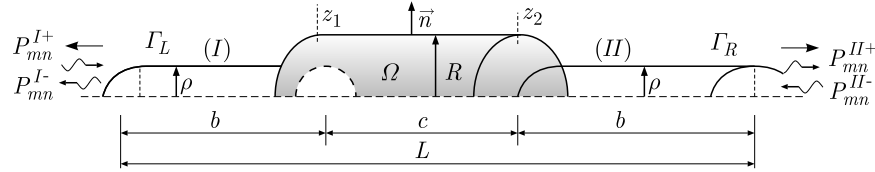

Fig. 2. Section with a duct diameter increase and then a sudden duct diameter decrease section

In the present study, we suppose that the abrupt change of the section is lined by a liner composed of a perforated plate and an absorbing porous material backed by a rigid plate. This liner is modeled later by its normalized acoustic impedance Z.

The multimodal scattering matrix is relating the out-coming modal pressures array

$$\mathbf{P}_{2N}^{out} = [P_{00}^{I-}, \dots, P_{mn}^{I-}, \dots, P_{PQ}^{I-}, P_{00}^{II+}, \dots, P_{mn}^{II+} \dots, P_{PQ}^{II+}]_N^{\mathrm{T}}$$

to the incoming modal pressures array

$$\mathbf{P}_{2N}^{in} = [P_{00}^{I+}, \dots, P_{mn}^{I+}, \dots, P_{PQ}^{I+}, P_{00}^{II-}, \dots, P_{mn}^{II-}, \dots, P_{PQ}^{II-}]_N^{\mathrm{T}}$$

as follows (Abom *et al.*, 1991; Taktak *et al.*, 2010)

$$\mathbf{P}_{2N}^{out} = \mathbf{S}_{2N \times 2N} \mathbf{P}_{2N}^{in} = \begin{bmatrix} \mathbf{R}_{N \times N}^{I} & \mathbf{T}_{I \to II \, N \times N} \\ \mathbf{T}_{II \to I \, N \times N} & \mathbf{R}_{N \times N}^{II} \end{bmatrix}_{2N \times 2N} \mathbf{P}_{2N}^{in} \qquad (2.1)$$

where m and n are respectively the circumferential and radial wave numbers, N is the number of propagating modes in both cross sections.

$R_{mn,pq}^{I}$ is the reflection coefficient of the wave incident to the element from side I, $T_{II \to I \, mn,pq}$ is the transmission coefficient of the wave from side II to side I, $R_{mn,pq}^{II}$ is the reflection coefficient of the wave incident to the element from side II and $T_{I \to II \, mn,pq}$ is the transmission coefficient of the wave from side I to side II.

The acoustical pressure p in the duct is obtained by solving the Helmholtz equation with the boundary conditions

$$
\begin{aligned}
k^2 p + \Delta p &= 0 && \text{for} && \Omega \\
\frac{\partial p}{\partial n_W} &= 0 && \text{for} && \Gamma_{WD} \\
Z \frac{\partial p}{\partial n_L} &= \mathrm{i}\omega\rho p && \text{for} && \Gamma_{LD}
\end{aligned}
\tag{2.2}
$$

k is the wave number, Ω is the acoustic domain inside the duct, Γ_{WD} and Γ_{LD} correspond to the rigid and lined walls, respectively, $\mathbf{n}_W$ and $\mathbf{n}_L$ are the normal vectors of these walls.

The corresponding weak variational formulation of the studied problem is

$$
\Pi = -\int_{\Omega} (\nabla q \cdot \nabla p)\, d\Omega + k^2 \int_{\Omega} qp\, d\Omega + \int_{\bigcup \Gamma_i} q \frac{\partial p}{\partial n_i}\, d\Gamma_i = 0
\tag{2.3}
$$

q is the test function, $d\Omega$ and $d\Gamma_i$ are the integration elements through the duct domain and boundaries, respectively, and $\bigcup \Gamma_i$ presents the whole boundary. The use of modal decomposition at left and right boundaries (Γ_L and Γ_R) introduces the modal pressures as additional degrees of freedom of the model as presented in the following expression

$$
\begin{aligned}
\int_{\Gamma_L} p J_m\Big(\frac{\chi_{mn}}{a} r\Big)\, d\Gamma_L &= (P_{mn}^{I+} + P_{mn}^{I-}) \int_{\Gamma_L} J_m\Big(\frac{\chi_{mn}}{a} r\Big)^2 r\, d\Gamma_L \\
\int_{\Gamma_R} p J_m\Big(\frac{\chi_{mn}}{a} r\Big)\, d\Gamma_R &= (P_{mn}^{II+} + P_{mn}^{II-}) \int_{\Gamma_R} J_m\Big(\frac{\chi_{mn}}{a} r\Big)^2 r\, d\Gamma_R
\end{aligned}
\tag{2.4}
$$

with a being the duct radius ($a = R$ or ρ) and r the radial coordinate.

The last integral of formulation (2.3) is given by the following expression by adding the modal incoming and outcoming pressures as additional degrees of freedom to the model

$$
\begin{aligned}
\int_{\bigcup \Gamma_i} q \frac{\partial p}{\partial n}\, d\Gamma &= \int_{\Gamma_t} q\Big(\frac{\mathrm{i}\omega\rho p}{Z}\Big)\, d\Gamma_{LD} + \sum_{n}^{N_r} \mathrm{i}k_{mn}\left[\left(n_L(P_{mn}^{I+} - P_{mn}^{I-}) \int_{\Gamma_L} q J_m(\chi_{mn} r)\, d\Gamma_L\right)\right. \\
&\left.+ \left(n_R(P_{mn}^{II+} - P_{mn}^{II-}) \int_{\Gamma_R} q J_m(\chi_{mn} r)\, d\Gamma_R\right)\right]
\end{aligned}
\tag{2.5}
$$

J_m is the Bessel function of the first kind of the order m, χ_{mn} is the nth root satisfying the radial hard-wall boundary condition on the wall of the main duct, r is the radial coordinate, $\mathbf{n}_L$ and $\mathbf{n}_R$ are the normal vectors.

For a fixed m, system (2.3) results in the following matrix system by taking into account the boundary conditions (Taktak *et al.*, 2010)

$$
\big[[q_1, \ldots, q_M], [1, \ldots, 1]\big]
\begin{bmatrix}
\mathbf{K} & \mathbf{E}_1 & \mathbf{E}_2 & \mathbf{F}_1 & \mathbf{F}_2 \\
\mathbf{G}_1 & \mathbf{G}_2 & \mathbf{G}_3 & \mathbf{0} & \mathbf{0} \\
\mathbf{0} & \mathbf{0} & \mathbf{0} & \mathbf{0} & \mathbf{0} \\
\mathbf{0} & \mathbf{0} & \mathbf{0} & \mathbf{0} & \mathbf{0} \\
\mathbf{H}_1 & \mathbf{0} & \mathbf{0} & \mathbf{H}_2 & \mathbf{H}_3
\end{bmatrix}
\left\{
\begin{array}{c}
\left\{\begin{array}{c} p_1 \\ \vdots \\ p_M \end{array}\right\} \\
\mathbf{P}_{mn}^{I-} \\
\mathbf{P}_{mn}^{I+} \\
\mathbf{P}_{mn}^{II-} \\
\mathbf{P}_{mn}^{II+}
\end{array}
\right\}
=
\left\{
\begin{array}{c}
\mathbf{0} \\
\vdots \\
\mathbf{0}
\end{array}
\right\}
\tag{2.6}
$$

M is the node number in the domain Ω, $\mathbf{K}$ is a matrix relating the test function to the nodal pressures in the domain, $\mathbf{E}_1$, $\mathbf{E}_2$, $\mathbf{F}_1$ and $\mathbf{F}_2$ are matrices relating the test function to the modal pressures on Γ_L and Γ_R, $\mathbf{G}_1$, $\mathbf{G}_2$ and $\mathbf{G}_3$ are matrices relating the nodal acoustic pressures in Ω to different modal pressures on the boundary Γ_L, $\mathbf{H}_1$, $\mathbf{H}_2$ and $\mathbf{H}_3$ are matrices relating the nodal acoustic pressures to different modal pressures on the boundary Γ_R.

The azimutal scattering matrix is written as

$$\boldsymbol{\Delta} = (\mathbf{V} - \mathbf{C}\mathbf{K}^{-1}\mathbf{B}^{-1})(\mathbf{U} - \mathbf{C}\mathbf{K}^{-1}\mathbf{A}^{-1}) \tag{2.7}$$

where $\mathbf{A}$, $\mathbf{B}$, $\mathbf{C}$, $\mathbf{U}$ and $\mathbf{V}$ are defined as

$$
\begin{aligned}
\mathbf{A} = \begin{bmatrix} \mathbf{E}_1 & \mathbf{F}_2 \end{bmatrix} \qquad & \mathbf{B} = \begin{bmatrix} \mathbf{E}_2 & \mathbf{F}_1 \end{bmatrix} \qquad && \mathbf{C} = \mathbf{G}_1 + \mathbf{H}_1 \\
\mathbf{U} = \begin{bmatrix} \mathbf{G}_2 & \mathbf{H}_3 \end{bmatrix} \qquad & \mathbf{V} = \begin{bmatrix} \mathbf{G}_3 & \mathbf{H}_2 \end{bmatrix} &&
\end{aligned}
\tag{2.8}
$$

The total scattering matrix $\mathbf{S}_{2N \times 2N}$ is achieved by repeating this operation for each m and by gathering the azimutal matrices $\boldsymbol{\Delta}_{2N_r \times 2N_r}$.

3.   Normalized acoustic impedance of the liner

In this study, a liner composed of a perforated plate and an absorbing porous material backed by a rigid plate is used. The normalized acoustic impedance of the liner is obtained as follows

$$Z = Z_{porous\ material} + Z_{perforated\ plate} \tag{3.1}$$

with

$$Z_{porous\ material} = Z_c \coth(jk_c d_m) \tag{3.2}$$

Z_c and k_c are the surface characteristic impedance and propagation constant of the porous material, respectively, and d_m is the material depth. The values of Z_c and k_c are estimated by the Delany-Bazley model (Delany and Bazley, 1970) expressed as follows

$$
\begin{aligned}
Z_c &= Z_0 \left[1 + 9.08 \left(\frac{f}{\sigma} \right)^{-0.754} - 11.9j \left(\frac{f}{\sigma} \right)^{-0.732} \right] \\
k_c &= \frac{\omega}{c_0} \left[1 + 10.8 \left(\frac{f}{\sigma} \right)^{-0.700} - 10.3j \left(\frac{f}{\sigma} \right)^{-0.595} \right]
\end{aligned}
\tag{3.3}
$$

where f is the frequency, σ is the flow resistivity, $Z_0 = \rho_0 c_0$ is the characteristic impedance of the air, ρ_0 is the air density, c_0 is the sound celerity in the air and ω is the pulsation ($\omega = 2\pi f$).

For the perforated plate, the acoustic impedance model of Elnady and Boden (2003) is used

$$Z_E = \mathrm{Re}\left\{ \frac{ik}{\sigma_p C_D} \left[\frac{t}{F(k'_s d_p/2)} + \frac{\delta_{re}}{F(k_s d_p/2)} \right] \right\} + \mathrm{iIm}\left\{ \frac{ik}{\sigma_p C_D} \left[\frac{t}{F(k'_s d_p/2)} + \frac{\delta_{im}}{F(k_s d_p/2)} \right] \right\} \tag{3.4}$$

with C_D being the discharge coefficient, d_p – pore diameter, t – plate thickness, σ_p – plate porosity, δ_{re} and δ_{im} – correction coefficients

$$
\begin{aligned}
\delta_{re} &= 0.2d_p + 200d_p^2 + 16000d_p^3 \qquad && \delta_{im} = 0.2856d_p \\
F(k_s d_p/2) &= 1 - \frac{J_1(k_s d_p/2)}{k_s \frac{d}{2} J_0(k_s d_p/2)} \qquad && F(k'_s d_p/2) = 1 - \frac{J_1(k'_s d_p/2)}{k'_s \frac{d}{2} J_0(k'_s d_p/2)} \\
k'_s &= \sqrt{\frac{-\mathrm{i}\omega}{\nu'}} \qquad k_s = \sqrt{-\frac{\mathrm{i}\omega}{\nu}} &&
\end{aligned}
\tag{3.5}
$$

with ν as the kinematic viscosity and

$$\nu' = 2.179\frac{\mu}{\rho_m} \tag{3.6}$$

where μ is the dynamic viscosity and ρ_m is the material density.

4. Computation of the acoustic power attenuation

The acoustic power attenuation W_{att} which is defined by the ratio between the incoming acoustic power W^{in} and the outcoming acoustic power W^{out} of the duct can be written as follows (Taktak *et al.*, 2010)

$$W_{att}(dB) = 10\log\frac{W^{in}}{W^{out}} = 10\log\frac{\sum\limits_{i=1}^{2N}|d_i|^2}{\sum\limits_{i=1}^{2N}\lambda_i|d_i|^2} \tag{4.1}$$

where λ_i and d_i are respectively the eigenvalues and the components of eigenvectors of the matrix $\mathbf{H}$ defined as follows

$$\mathbf{H}_{2N\times2N} = \mathbf{S'}_{2N\times2N}^{\mathrm{T}*}\mathbf{S'}_{2N\times2N} \qquad \mathbf{S'}_{2N\times2N} = \mathbf{X}_{2N\times2N}\mathbf{S}_{2N\times2N}\mathbf{X}_{2N\times2N}^{-1}$$

$$\mathbf{X}_{2N\times2N} = \begin{bmatrix} \left[\mathrm{diag}\left(\sqrt{N_{mn}k_{mn}/(2\rho_0c_0k)}\right)\right]_{N\times N} & \mathbf{0}_{N\times N} \\ \mathbf{0}_{N\times N} & \left[\mathrm{diag}\left(\sqrt{N_{mn}k_{mn}/(2\rho_0c_0k)}\right)\right]_{N\times N} \end{bmatrix} \tag{4.2}$$

with

$$N_{00} = 1 \qquad N_{mn} = SJ_m^2(\chi_{mn})\left(1 - \frac{m^2}{\chi_{mn}^2}\right) \tag{4.3}$$

where $S = \pi a^2$ is the cross section area, and

$$k_{mn} = \sqrt{k^2 - \left(\frac{\chi_{mn}}{a}\right)^2} \tag{4.4}$$

where k_{mn} is the axial wave number associated to the mode (m,n) in the main duct.

5. Numerical results

The characteristics of the used liner are:

- The perforated plate: thickness $e = 1\,\mathrm{mm}$, hole diameter $d_p = 1\,\mathrm{mm}$ with a perforation ratio $\sigma_p = 2.5\%$.
- The porous material: thickness $d_m = 20\,\mathrm{mm}$ and the flow resistivity $\sigma = 26000\,\mathrm{Nsm}^{-1}$.
- The rigid wall plate.

The acoustic impedance computed using these characteristics according to the Delany and Bazley (1970) model is then used as an input for computation of the numerical multimodal scattering matrix and the acoustic power attenuation of the studied ducts. The effect of two geometrical parameters is studied: the length and the radius of the section change.

5.1. Duct having a diameter decrease

In this part, the case presented in Fig. 1 is treated: the duct presents a diameter decrease characterized with length equal to c and radius equal to ρ. This part of the duct is lined with the studied liner. In the following, the ffect of change of these parameters is investigated.

5.1.1. Effect of change in length

The scattering matrix coefficients and the acoustic power attenuation are calculated in the cases of wall and lined ducts having a duct diameter decrease in order to determine the influence of duct diameter decrease part length on its acoustic behavior. The duct has 0.05 m radius and length of 1 m. The duct diameter decrease is 0.025 m. Fourth configurations of the ducts are studied:

- First configuration: the length of the duct is divided into three portions: $b = 0.4$ m and $c = 0.2$ m, which makes the percentage of the duct diameter decrease portion equal to 20%.
- Second configuration: the length of the duct is divided into three portions: $b = 0.3$ m and $c = 0.4$ m, which makes the percentage of the duct diameter decrease portion equal to 40%.
- Third configuration: the length of the duct is divided into three portions: $b = 0.2$ m, $c = 0.6$ m, which makes the percentage of the duct diameter decrease portion equal to 60%.
- Fourth configuration: the length of the duct is divided into three portions: $b = 0.1$ m, $c = 0.8$ m, which makes the percentage of the duct diameter decrease portion equal to 80%.

The reflection coefficients $R_{00,00}$ with and without the liner have the same shape (Fig. 3), except that in the treated length these coefficients are significantly attenuated. Note that all $R_{10,10}$ (Fig. 4) are equal to zero except for the forth configuration for values of k_a ranging 2.5 to 3.8 when not treated. On the other hand, $R_{20,20}$ reflection coefficients do not show a difference for the treated or not treated length.
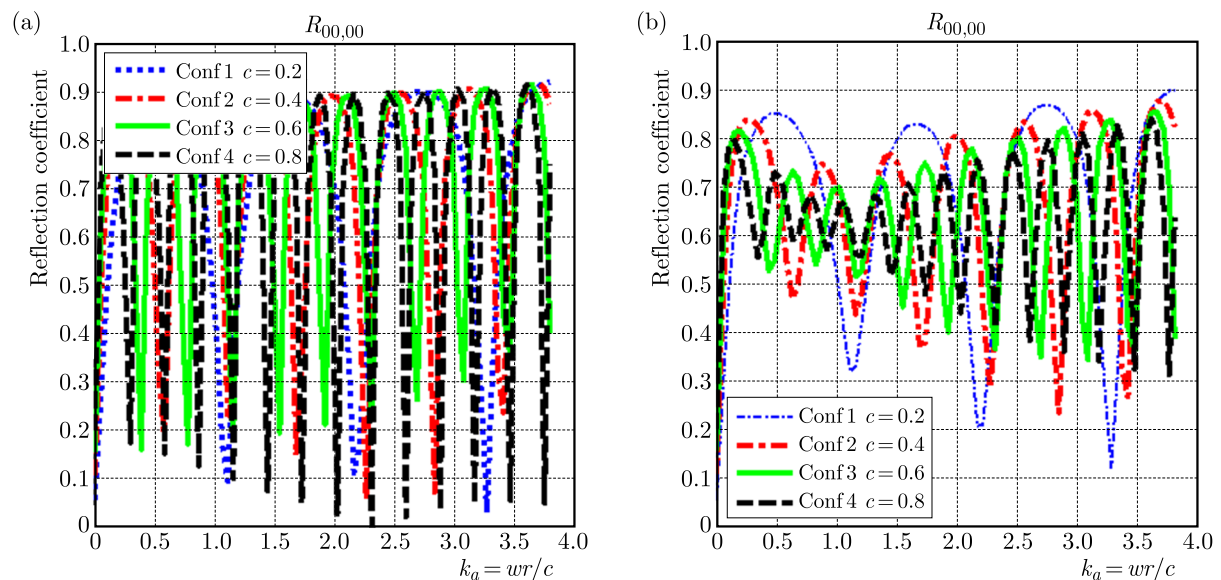

Fig. 3. Reflection coefficient $R_{00,00}$ versus k_a for several configurations. Duct diameter decrease case (a) without liner, (b) with liner

The more the length of the duct diameter decrease increases, the more the transmission decreases and the transmission decreases as the attenuation increases. Note that all transmissions $T_{10,10}$ and $T_{20,20}$ in the free driving material are equal to zero throughout the frequency range studied (no transmission according to both directions of wave propagation) except for $T_{00,00}$
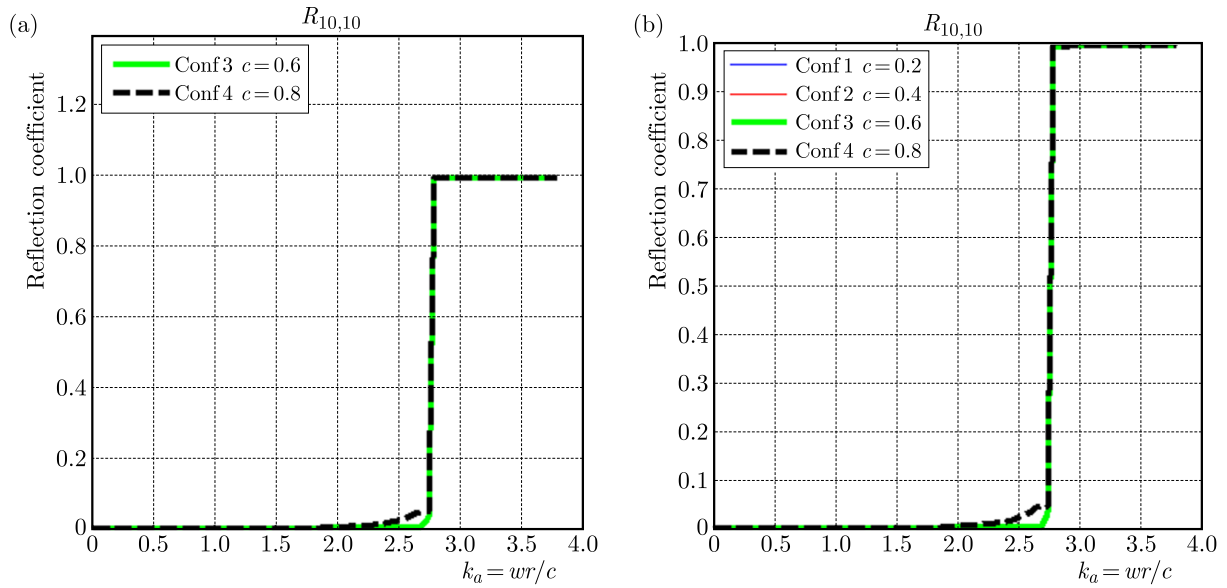
Fig. 4. Modulus of the reflection coefficient $R_{10,10}$ versus k_a for several configurations. Duct diameter decrease case (a) without liner, (b) with liner
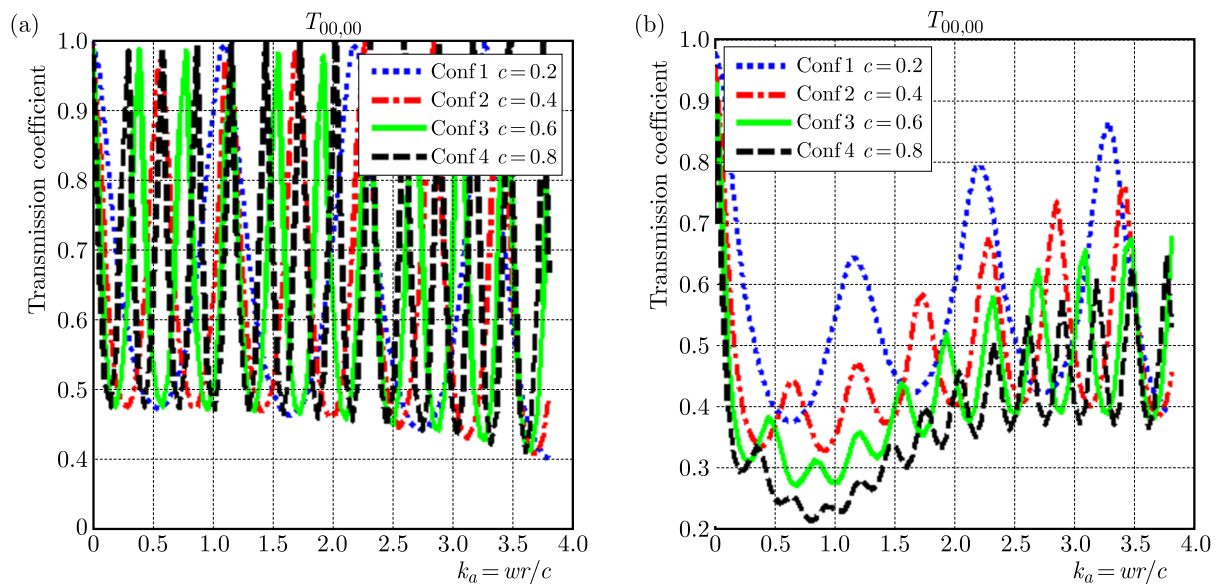

Fig. 5. Modulus of the transmission coefficient $T_{00,00}$ versus k_a for several configurations. Duct diameter decrease case (a) without liner, (b) with liner

transmission submitting a response for values of k_a ranging $[0, 4]$. For $T_{00,00}$ (Fig. 5), all configurations exhibit harmony behavior for k_a ranging from 0 to 4. Figure 6 presents the acoustic power attenuation of the studied cylindrical duct versus k_a for different studied configurations. The results show that attenuation reaches a maximum near k_a equal 2.5. The amplitude of this maximum is about $4.8\,\mathrm{dB}$, $4.3\,\mathrm{dB}$, $4\,\mathrm{dB}$ and $3\,\mathrm{dB}$ for the fourth, third, second and first configuration, respectively. These figures show more clearly that the length of the duct diameter decrease increases more than the attenuation increases. In terms of materials without reflection, the more the length of the duct diameter decrease increases, the more the reflections decrease. The unreflective wave will be absorbed. For the treated length, the unreflective wave will be partly absorbed and the rest part refracted. The more the length of the duct diameter decrease increases (from the fourth to first configuration), the more the large part of the wave will be
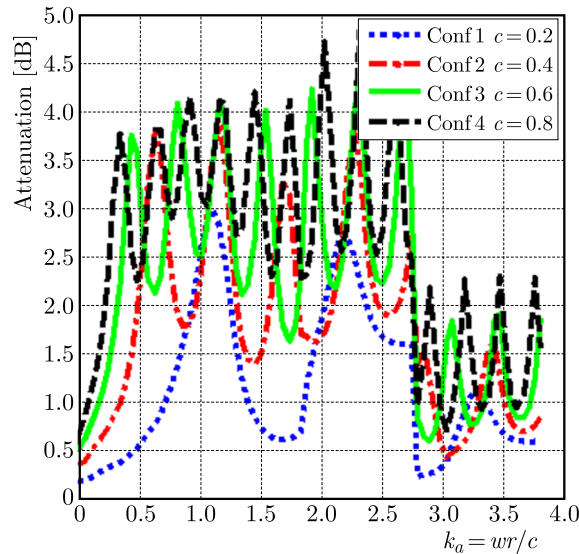
Fig. 6. Acoustic attenuation versus k_a for several configurations. Duct diameter decrease with liner

absorbed. This seems logical as the more the length of the duct diameter decrease increases, the more the surface of the material increases, and the absorption is greater.

5.1.2. Effect of the variation of the radius

The scattering matrix coefficients and the acoustic power attenuation are calculated in the cases of wall and lined ducts having a duct diameter decrease in order to determine the influence of the duct diameter decrease part radius on its acoustic behavior. The duct has 0.05 m in radius and length of 1 m. The length of the duct is divided into three portions: the rigid length is equal to 0.35 m, the length treated is 0.3 m, the rigid length is equal to 0.35 m. Fourth configurations of ducts are studied:

- First configuration: the radius of duct diameter decrease is 0.04 m, which makes a radius reduction of 20%.

- Second configuration: the radius of duct diameter decrease is 0.03 m, which makes a radius reduction of 40%.

- Third configuration: the radius of duct diameter decrease is 0.02 m, which makes a radius reduction of 60%.

- Fourth configuration: the radius of duct diameter decrease is 0.01 m, which makes a radius reduction of 80%.

The radius variation affects the amplitude of the reflection coefficients. The reflection modules have a good harmony for all configurations for k_a values $[0, 4]$. It is noted that configurations 3 and 4 (Fig. 7) show good attenuation in the case of treated conduct. The reflection module $R_{10,10}$ shows no change for the first configuration (with and without material), for configuration 3 against improved significantly in the case of the treated conduct going from $k_a = 0$ to 2.6 (Fig. 8). For a more increase of the duct diameter decrease, the transmission decreases (0.9 dB to 0.1 dB). For the fourth configuration, the attenuation of the transmission is 65% near k_a equal 0.75 (Fig. 9). The four configurations have a good harmony for k_a ranging from 0 to 4. The modulus of transmission $T_{10,10}$ and $T_{20,20}$ is zero for the second and third configuration, leading to say that the length treated has no effect contrary to configurations 1 and 2 (Fig. 10) in with the liner of conduct has a considerable effect.
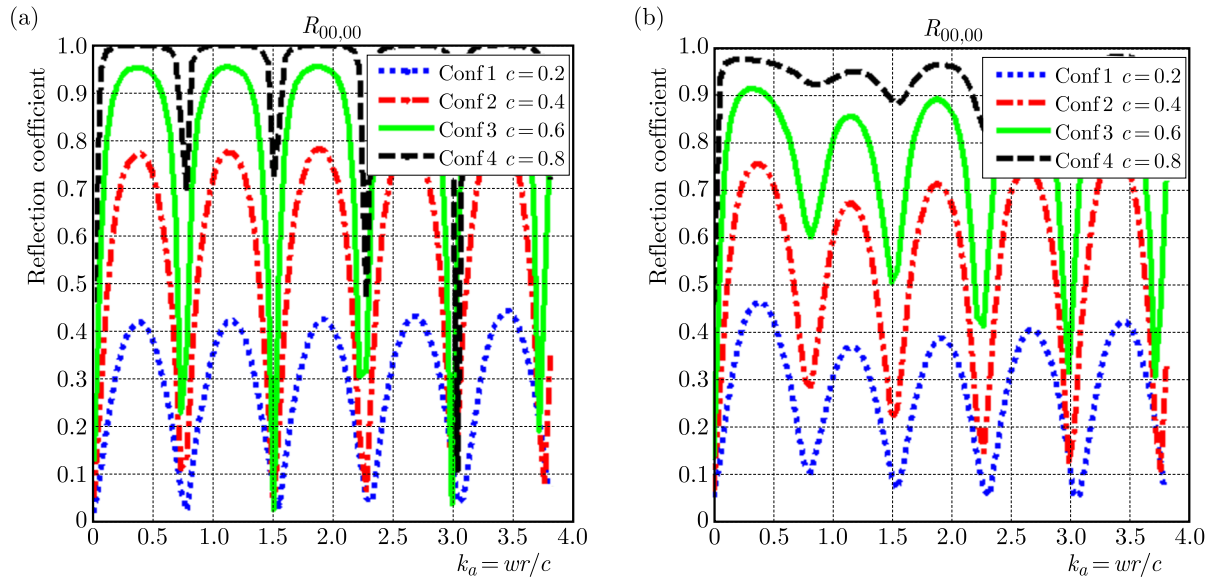
Fig. 7. Modulus of the reflection coefficient $R_{00,00}$ versus k_a for several configurations. Duct diameter decrease case (a) without liner, (b) with liner
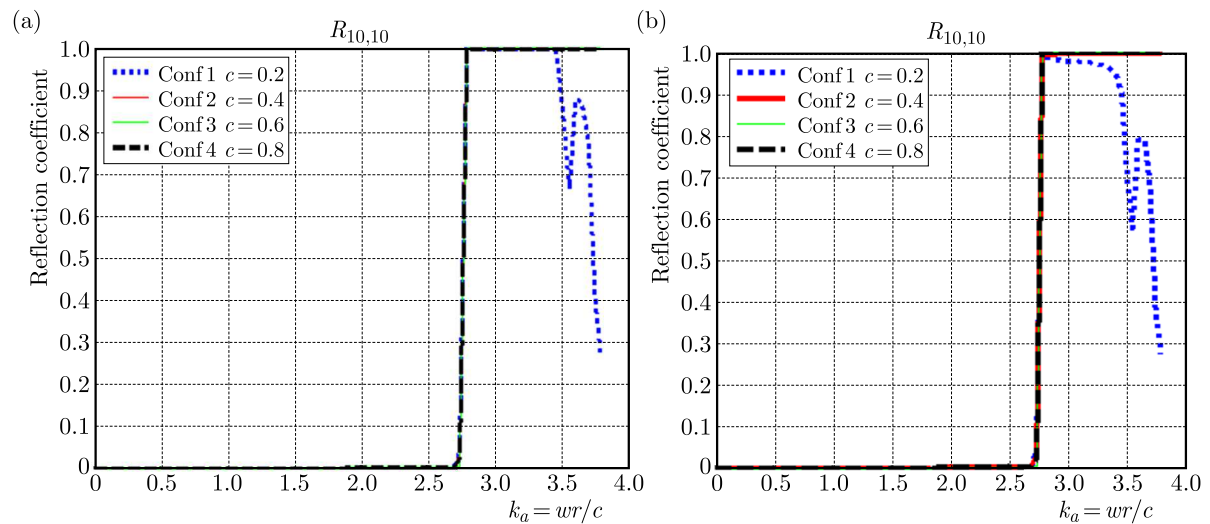

Fig. 8. Modulus of the reflection coefficient $R_{10,10}$ versus k_a for several configurations. Duct diameter decrease case (a) without liner, (b) with liner

5.2. Duct with a diameter increase

In this part, the case presented in Fig. 2 is treated: the duct presents a diameter increase characterized with length equal to c and radius equal to ρ. This part of the duct is lined with the studied liner. In the following, the effect of changing these parameters is investigated.

5.2.1. Effect of change in length

The scattering matrix coefficients and the acoustic power attenuation are calculated in the cases of rigid and lined ducts having a diameter increase in order to determine the influence of duct diameter increase part length on its acoustic behavior. The duct is $0.05\,\mathrm{m}$ in radius and length of $1\,\mathrm{m}$. The duct diameter increase amounts to $0.1\,\mathrm{m}$. Fourth configurations of ducts are studied:
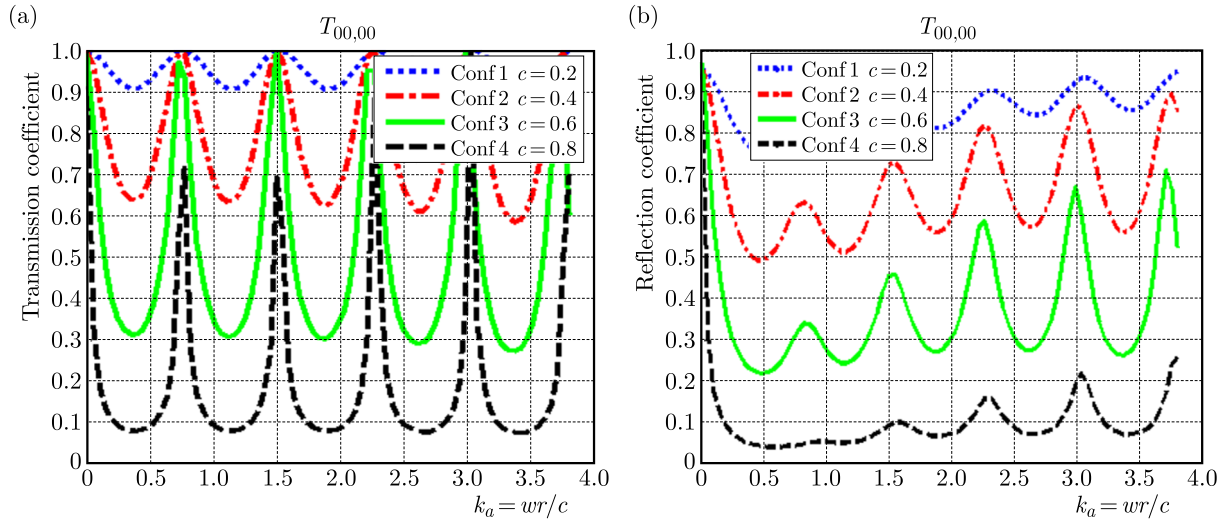
(a)

(b)

Fig. 9. Modulus of the transmission coefficient $T_{00,00}$ versus k_a for several configurations. Duct diameter decrease case (a) without liner, (b) with liner
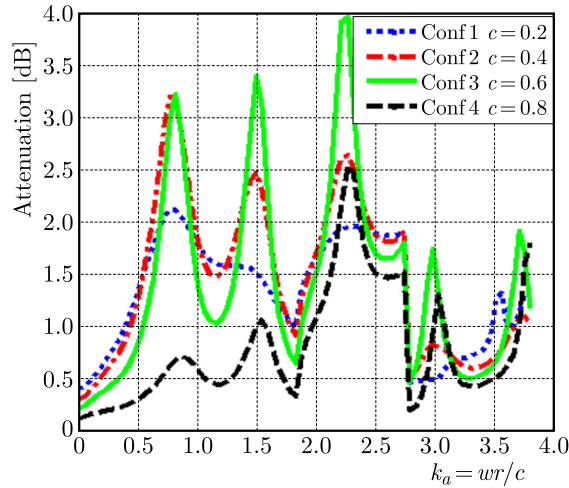

Fig. 10. Acoustic attenuation versus k_a for several configurations

- First configuration: the length of the duct is divided into three portions: $b = 0.4\,\mathrm{m}$ and $c = 0.2\,\mathrm{m}$, which makes the percentage of the duct diameter decrease portion equal to 20%.

- Second configuration: the length of the duct is divided into three portions: $b = 0.3\,\mathrm{m}$ and $c = 0.4\,\mathrm{m}$, which makes the percentage of the duct diameter decrease portion equal to 40%.

- Third configuration: the length of the duct is divided into three portions: $b = 0.2\,\mathrm{m}$, $c = 0.6\,\mathrm{m}$, which makes the percentage of the duct diameter decrease portion equal to 60%.

- Fourth configuration: the length of the duct is divided into three portions: $b = 0.1\,\mathrm{m}$, $c = 0.8\,\mathrm{m}$, which makes the percentage of the duct diameter decrease portion equal to 80%.

Figures 11 and 12 present the variation of the modulus of reflection coefficients $R_{00,00}$ and $R_{10,10}$ versus k_a, whereas Figs, 13 and 14 present the variation of the modulus of transmission coefficients $T_{00,00}$ and $T_{10,10}$ versus k_a for several studied configurations. One can observe that the more the length of duct diameter decrease increases, the more transmission decreases and the transmission decreases as the attenuation increases. This is presented in Fig. 15 which shows that the attenuation has a maximum when the transmission is low. Indeed, the fourth configuration has an attenuation of 2 dB for $k_a = 2.5$. In the case without materials, there is no attenuation.
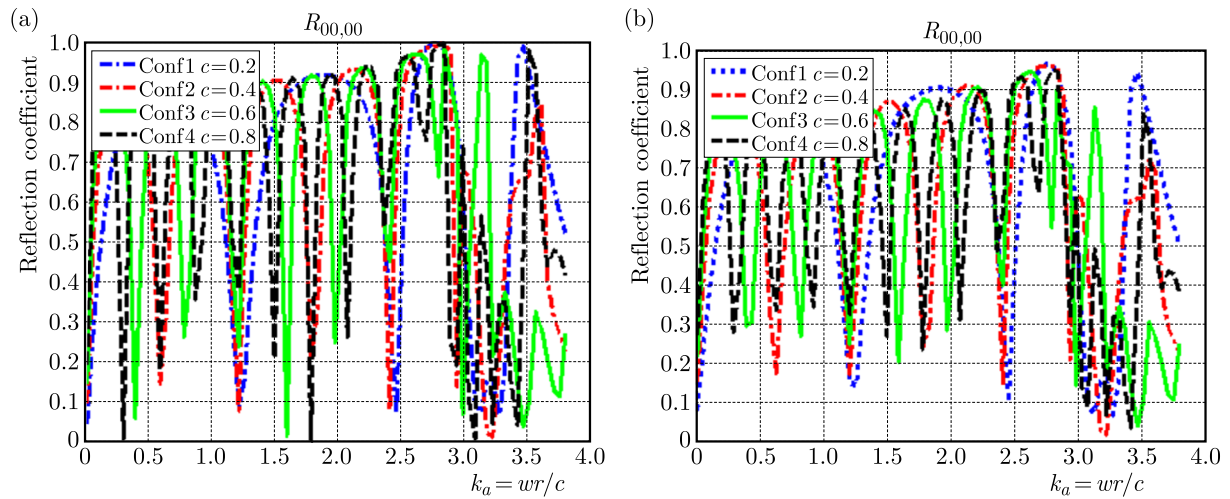
Fig. 11. Modulus of the reflection coefficient $R_{00,00}$ versus k_a for several configurations. Duct diameter increase case (a) without liner, (b) with liner
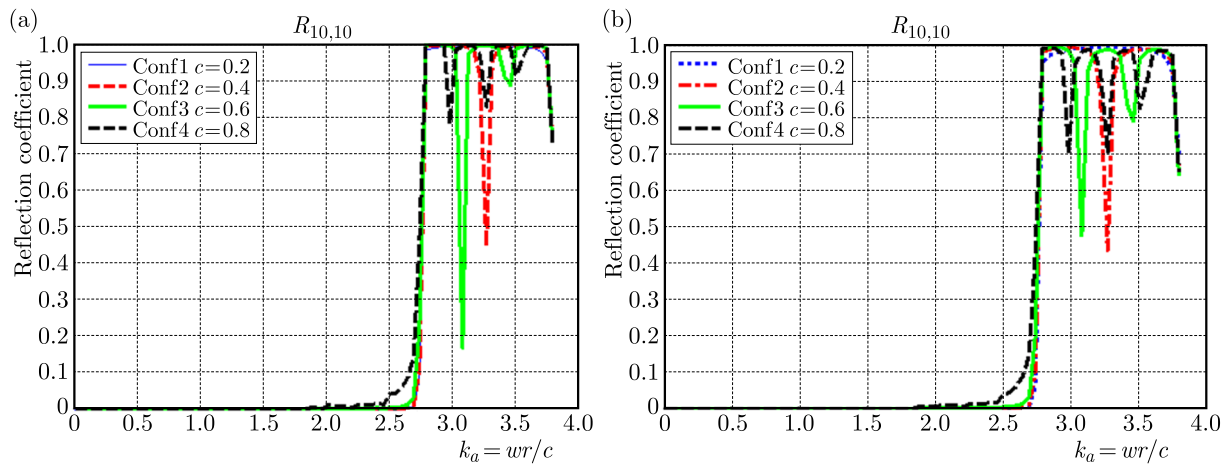

Fig. 12. Modulus of the reflection coefficient $R_{10,10}$ versus k_a for several configurations. Duct diameter increase case (a) without liner, (b) with liner
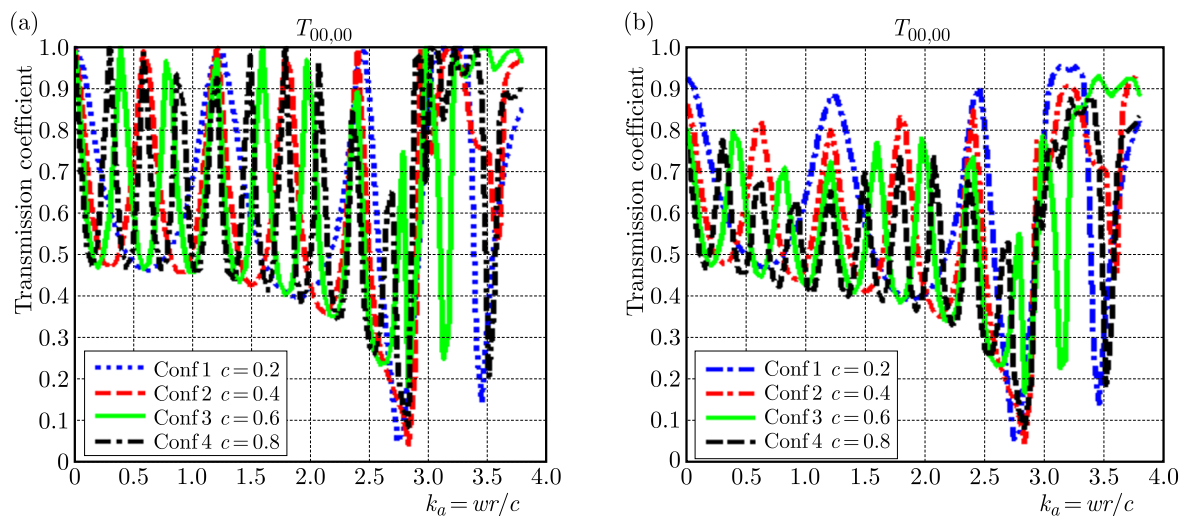

Fig. 13. Modulus of the transmission coefficient $T_{00,00}$ versus k_a for several configurations. Duct diameter increase case (a) without liner, (b) with liner
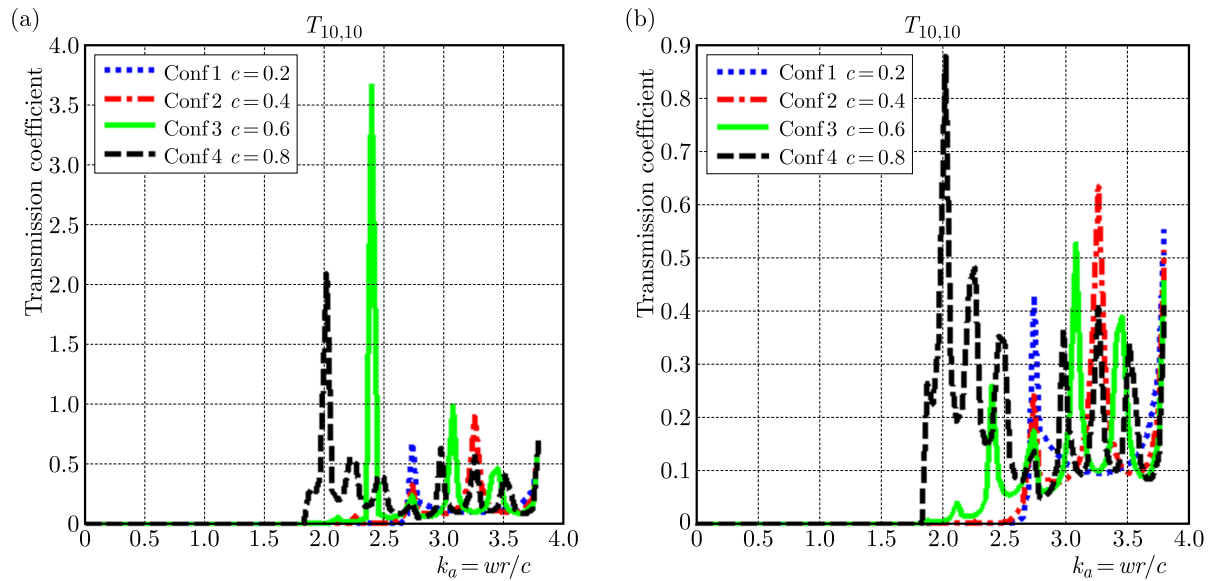
(a)

(b)

Fig. 14. Modulus of the transmission coefficient $T_{10,10}$ versus k_a for several configurations. Duct diameter increase case (a) without liner, (b) with liner
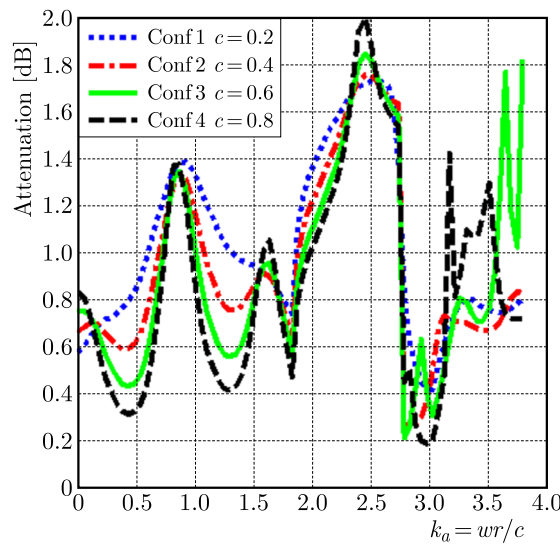

Fig. 15. Acoustic attenuation versus k_a for several configurations (duct diameter increase with liner)

5.2.2. Effect of variation of radius

The scattering matrix coefficients and the acoustic power attenuation are calculated in the cases of rigid and lined ducts having a diameter increase in order to determine the influence of the duct diameter increase on its acoustic behavior. The duct has radius of $0.05\,\mathrm{m}$ and length of $1\,\mathrm{m}$. The length of the duct is divided into three portions. The rigid length is equal to $0.35\,\mathrm{m}$, the length treated is $0.3\,\mathrm{m}$ and the rest rigid length is equal to $0.35\,\mathrm{m}$. Fourth configurations of ducts are studied:

- First configuration: the duct diameter increase is $0.06\,\mathrm{m}$ which makes an increase in radius equal to 20%.

- Second configuration: the duct diameter increase is $0.07\,\mathrm{m}$ which makes an increase in radius equal to 40%.

- Third configuration: the duct diameter increase is $0.08\,\mathrm{m}$ which makes an increasee in radius equal to 60%.

- Fourth configuration: the duct diameter increase is $0.09\,\mathrm{m}$ which makes an increase in radius equal to 80%.

Figures 16, 17 present the variation of the modulus of reflection coefficients $R_{00,00}$ and $R_{10,10}$ versus k_a, whereas Figs. 18 and 19 present the variation of the modulus of transmission coefficients $T_{00,00}$ and $T_{10,10}$ versus k_a for several studied configurations. From these figures it can be concluded that the more the duct diameter increases, the more transmission decreases and the reflection increases. There is not much difference in the transmission in the case of conduct treated materials (it falls slightly from 1 to 0.9). Figure 20 presents the acoustic attenuation of the four studied cases. The fourth configuration is the more absorbent with a maximum of $2\,\mathrm{dB}$ at $k_a = 2.5$. This leads to say that the duct diameter decrease configuration is more absorbent, therefore, more efficient than the configuration with the duct diameter increase. Indeed, the configuration with the duct diameter increase section shows no great reflection (low values for $R_{00,00}$ and $R_{10,10}$).
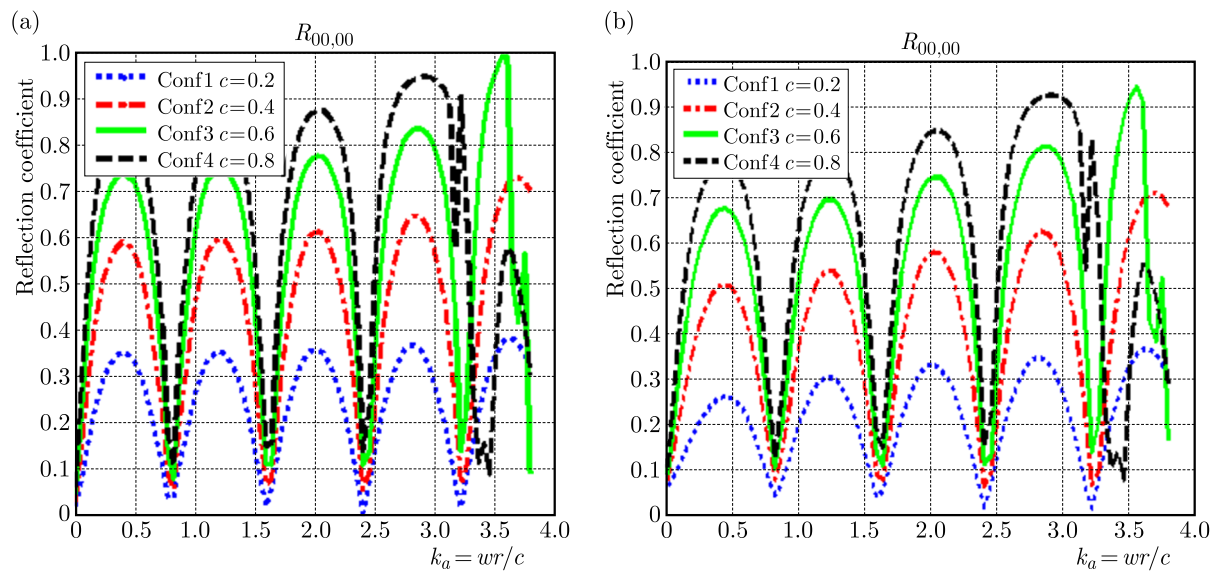

Fig. 16. Modulus of the reflection coefficient $R_{00,00}$ versus k_a for several configurations. Duct diameter increase case (a) without liner, (b) with liner
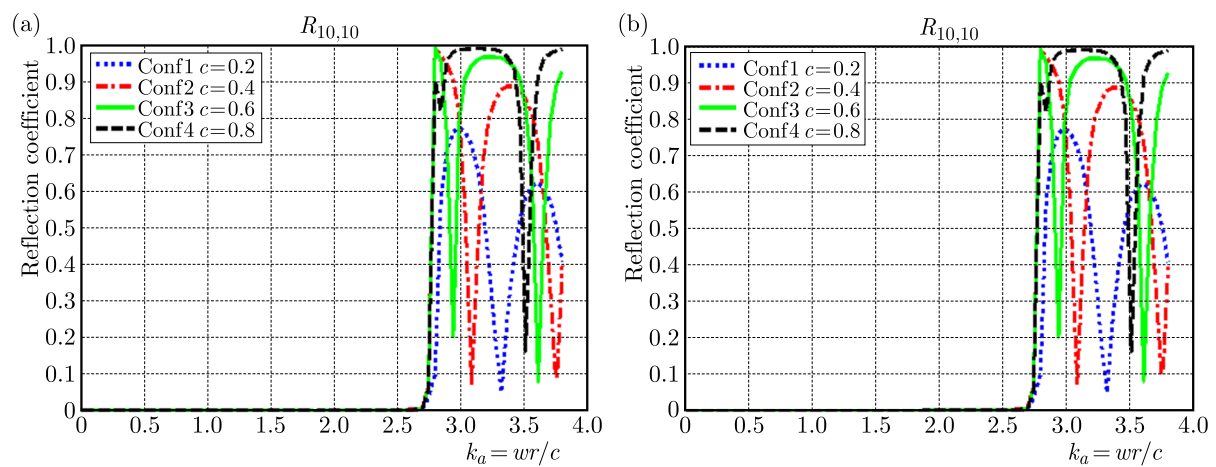

Fig. 17. Modulus of the reflection coefficient $R_{10,10}$ versus k_a for several configurations. Duct diameter increase case (a) without liner, (b) with liner
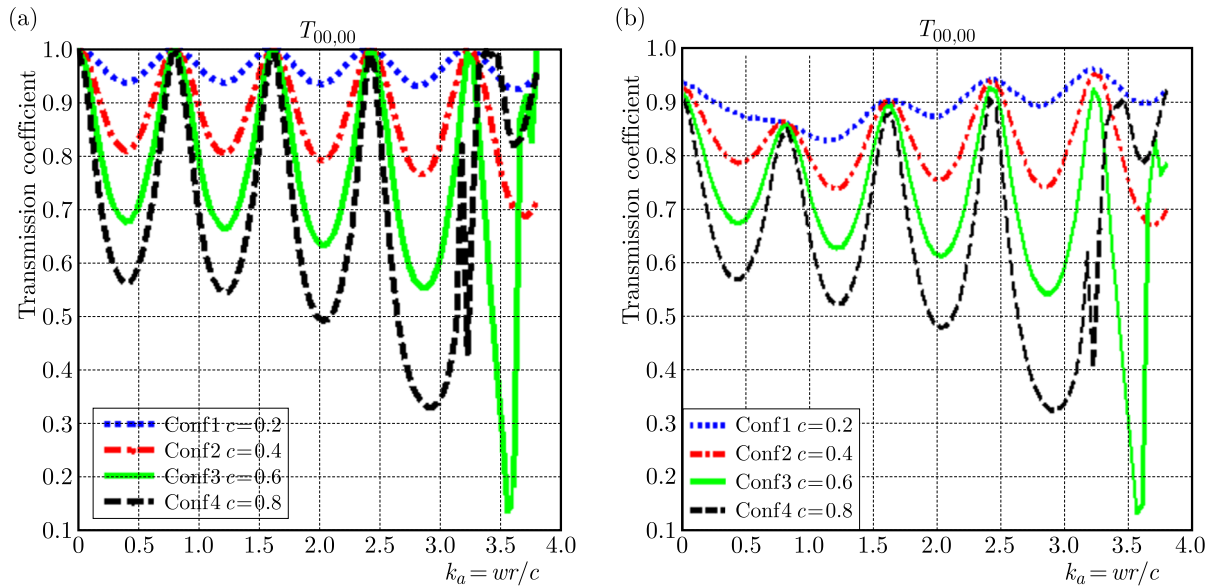
Fig. 18. Modulus of the transmission coefficient $T_{00,00}$ versus k_a for several configurations. Duct diameter increase case (a) without liner, (b) with liner
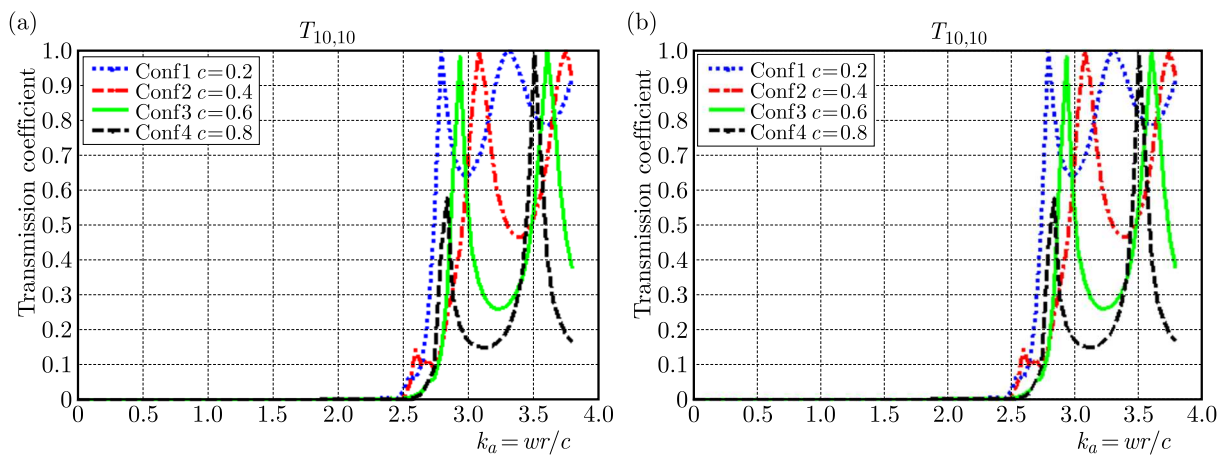

Fig. 19. Modulus of the transmission coefficient $T_{10,10}$ versus k_a for several configurations. Duct diameter increase case (a) without liner, (b) with liner
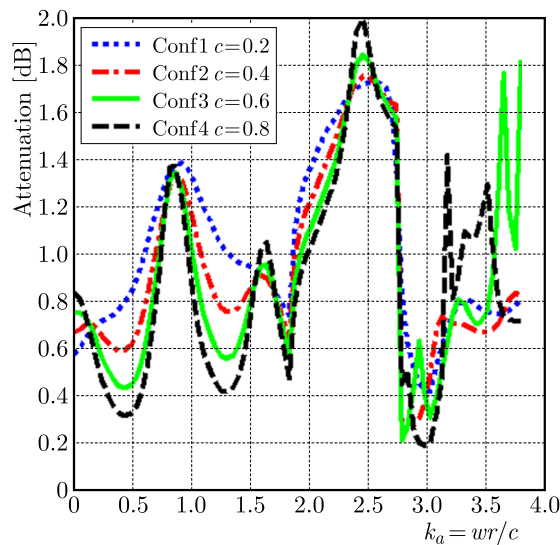

Fig. 20. Acoustic attenuation versus k_a for several configurations (duct diameter increase with liner)

6. Conclusions

In this paper, effect of geometry and impedance variation on the Acoustic Performance of Porous Material Lined Duct is studied. The main conclusions drawn from the study are as follows:

For the case of duct diameter decrease:

- The more the length of the duct diameter decrease increases, the more attenuation increases.

- In terms of materials, the more the length of duct diameter decrease increases, the more reflections decreases and the unreflective wave is absorbed.

- For the treated length, the unreflective wave will be partly absorbed and the rest part refracted. The more the length of duct diameter decrease increases, the more the wave is absorbed.

- The more the length of the duct diameter decrease increases, the more the surface of the material increases, and the absorption is greater.

- The radius variation affects the amplitude of the reflection coefficients. The more the duct diameter decrease increases, the more the transmission decreases.

For the case of duct diameter increase:

- The more the length of the duct diameter increase increases, the more the transmission decreases and the transmission decreases, the more the attenuation increases.

- With the treated length, the more the radius of the duct diameter increase increases, the more reflection increases and the reflection increases, the more the transmission decreases. There is not much difference transmission.

It is concluded from the results presented above that the duct diameter decrease configuration is more absorbent, therefore, more efficient than the configuration with the duct diameter increase.

References

1. ABOM M., 1991, Measurement of the scattering matrix of acoustical two-ports, *Mechanical Systems Signal Processing*, **5**, 2, 89-104

2. AURÉGAN Y., STAROBINSKI R., 1998, Determination of acoustical energy dissipation/production potentiality from the acoustic transfer functions of a multiport, *Acta Acustica United with Acustica*, **85**, 788-792

3. BEN JDIDIA M., AKROUT A., TAKTAK M., HAMMAMI L., HADDAR M., 2014, Thermal effect on the acoustic behavior of an axisymmetric lined duct, *Applied Acoustics*, **86**, 138-145

4. BI W.P., PAGNEUX V., LAFARGE D., AURÉGAN Y., 2006, Modelling of sound propagation in non-uniform lined duct using a multi-modal propagation method, *Journal of Sound and Vibration*, **289**, 1091-1111

5. DELANY M.E., BAZLEY E.N., 1970, Acoustical properties of fibrous absorbent materials, *Applied Acoustics*, **3**, 105-116

6. ELNADY T., BODEN H., 2003, On semi-empirical liner impedance modeling with grazing flow, *Proceedings of 9th AIAA/CEAS Aeroacoustics Conference*, U.S.A.

7. LEROUX M., JOB S., AURÉGAN Y., PAGNEUX V., 2003, Acoustical propagation in lined duct with flow. Numerical simulations and measurements, *10th International Congress of Sound and Vibration*, Stockholm, Sweden, 3255-3262

8. SITEL A., VILLE J.M., FOUCART F., 2006, Multimodal procedure to measure the acoustic scattering matrix of a duct discontinuity for higher order mode propagation conditions, *Journal of the Acoustical Society of America*, **120**, 5, 2478-2490

9. TAKTAK M., MAJDOUB M.A., BENTAHAR M., HADDAR M., 2012, Numerical modelling of the sound propagation in axisymmetric lined flow duct, *Archives of Acoustics*, **37**, 2, 151-160

10. TAKTAK M., MAJDOUB M.A., BENTAHAR M., HADDAR M., 2013, Numerical characterization of an axisymmetric lined duct with flow using multimodal scattering matrix, *Journal of Theoretical and Applied Mechanics*, **51**, 2, 313-325

11. TAKTAK M., VILLE J.M., HADDAR M., GABARD G., FOUCART F., 2010, An indirect method for the characterization of locally reacting liners, *Journal of the Acoustical Society of America*, **127**, 6, 3548-3559